

# On the problem of natural convection in liquid phase thermotransport coefficients measurements

Cite as: Physics of Fluids 9, 510 (1997); <https://doi.org/10.1063/1.869215>

Submitted: 11 June 1996 • Accepted: 16 October 1996 • Published Online: 04 June 1998

J. P. Garandet, J. P. Praizey, S. Van Vaerenbergh, et al.



View Online



Export Citation

## ARTICLES YOU MAY BE INTERESTED IN

[Thermophobicity of liquids: Heats of transport in mixtures as pure component properties—The case of arbitrary concentration](#)

The Journal of Chemical Physics **141**, 134503 (2014); <https://doi.org/10.1063/1.4896776>

[Numerical simulations of the translational and shape oscillations of a liquid drop in an acoustic field](#)

Physics of Fluids **9**, 519 (1997); <https://doi.org/10.1063/1.869216>

[Linear stability and transient growth in driven contact lines](#)

Physics of Fluids **9**, 530 (1997); <https://doi.org/10.1063/1.869217>

APL Machine Learning

Open, quality research for the networking communities

MEET OUR NEW EDITOR-IN-CHIEF

LEARN MORE



# On the problem of natural convection in liquid phase thermotransport coefficients measurements

J. P. Garandet and J. P. Praizey

*Commissariat à l'Energie Atomique, DTA/CEREM/DEM/SES, Centre d'Etudes Nucleaires de Grenoble, 38054 Grenoble Cedex 9, France*

S. Van Vaerenbergh

*Université Libre de Bruxelles/Service Chimie Physique, 50 Avenue F. D. Roosevelt, 1050 Bruxelles, Belgium*

T. Alboussiere

*Laboratoire EPM/Madylam, CNRS UPR A 9033, ENSHMG, BP 95, 38402 St. Martin d'Heres Cedex, France*

(Received 11 June 1996; accepted 16 October 1996)

We focus in this paper on the effect of natural convection in thermodiffusion coefficients measurements in liquid metal alloys both for normal and microgravity conditions. Our previous experimental results are briefly recalled, with a special emphasis on the data recently obtained from the EURECA space mission. With respect to the ground based values, it is seen that the solutal separation is always significantly higher in microgravity, even in systems where solutal stabilization of the flow has an effect. Simple scaling analysis arguments show that the error induced by additional convective transport scales with the square of the fluid velocity. Such a result compares favorably with existing three dimensional (3D) numerical data. The theory also accounts qualitatively for the reduced separation observed experimentally in ground based set-ups. We conclude that it is in principle possible to perform accurate measurements in space, but that the size of the capillaries used in the experiments should always be limited to roughly two millimeters. On Earth on the other hand, the risk of convective interference cannot be avoided. © 1997 American Institute of Physics. [S1070-6631(97)00403-0]

## I. INTRODUCTION

The modellization and the understanding of a variety of processes rely on the knowledge of transfer coefficients. However, an accurate measurement of these parameters is very difficult when the diffusivities are very low, e.g., for the case of solute transport in liquid metals or semiconductors. Indeed, the unavoidable natural convection induced by the cross product interaction of density gradients with gravity may lead to significant errors, even in thin capillaries.

A pendent question is thus to assess the possibility of realizing these measurements on Earth, the alternative being to carry out the experiments aboard space vehicles where the intensity of gravity is reduced by a factor ranging from  $10^4$  to  $10^6$ . Our purpose in this paper is to provide some new insights to this problem for the case of thermodiffusion coefficients measurements (Soret effect).

In a typical long capillary or shear cell set-up, the metallic sample is melted and submitted to an axial thermal gradient for a sufficiently long time to allow a steady-state to be reached. A tricky part in the procedure consists in avoiding any altering of the liquid state solute distribution during the solidification phase. The thermotransport coefficient is then deduced from an analysis of the temperature/composition profiles in the resulting solid sample.

Since the axial component of the density (thermal and/or solutal) gradient is generally much larger than the lateral component, the experimental set-up is maintained vertical for ground configurations. In space, the cavity should be considered horizontal for modelling purposes since there is al-

ways a component of the residual gravity that is transverse to the capillary axis and thus provides the most effective driving force for convection. The full three dimensional numerical analysis of the problem has been carried out by Henry and Roux for both the horizontal<sup>1</sup> and the inclined<sup>2</sup> configurations.

Away from the endwalls, the numerical solutions exhibit a parallel flow behavior, which inspired Jacqmin's analytical approach.<sup>3</sup> A striking result of the simulations is that the solute gradient around the central part of the cavity correlated univocally with the maximum convective velocity. As the measured thermodiffusion coefficient is deduced directly from the composition profile, this means that the final result depends on neither the physical driving force (thermal and/or solutal gradients) nor on the detailed shape of the flow field.<sup>1</sup>

This point is very important for our present purposes since it can be thought that an effective diffusivity concept can capture the essence of the transport problem, as done in a previous work for an isothermal diffusion coefficients configuration.<sup>4</sup> From a simple order of magnitude analysis, carried out in parallel with numerical simulations, we showed that the error induced by convection was proportional to the square of the average fluid flow velocity  $\bar{W}$ .

More precisely, the effective diffusion coefficient  $D^*$ , i.e., the one that would be deduced from the experimental data assuming purely diffusive transport, was seen to be related to the true diffusion coefficient  $D$  by

$$D^* = D[1 + \alpha \bar{W}^2 H^2 / D^2], \quad (1)$$

$H$  being a typical dimension of the cavity and  $\alpha$  a proportionality factor predicted to be of order of magnitude 1/4 by the scaling analysis. A derivation of Eq. (1) is proposed in the Appendix.

One of the purposes of the present work is to adapt the above result to the thermodiffusion problem, and to see how this effective diffusivity approach compares with the Henry and Roux numerical results. Also interesting for the validation of the effective diffusivity concept is the existence of experimental data for Soret coefficients in tin based alloys both on the ground and in microgravity.

Microgravity results were obtained during Spacelab missions on the NASA shuttle during the FSLP (1983) and D1 (1985) flights,<sup>5</sup> as well as on the recent EURECA automatic platform (1992). When the same experiments were run on Earth, the observed chemical separation was always smaller, but it had been conjectured<sup>5</sup> that solutal stabilization of the flow could be efficient enough to guarantee purely diffusive transport conditions. To gain some insights into this important question, we shall have to consider the origin of possible convective movements in Earth based conditions.

For instance, a slight misalignment of the capillary axis with the vertical direction can lead to fluid flows that can significantly modify the transport conditions. Another possible driving force for fluid flow is the existence of radial temperature differences in the sample due to global heat transfer in the furnace. Both causes may be expected to have an impact on the separation process, and we shall try to correlate our experimental data with the numerical results taking into account the mechanism of solutal stabilization of convection as discussed by Hart.<sup>6</sup>

We present in Sec. II the various possible formulations of the thermodiffusion problem, derive the effective diffusivity relation scaling the error induced by convective transport and compare its predictions with the numerical data. Section III is devoted to the experimental procedure and results, with special emphasis on the information gained during the EURECA mission. The possibility of realizing Soret coefficient measurements in space is discussed in Sec. IV. Finally, we analyze in Sec. V the differences between ground based and space results in liquid metals or semiconductors.

## II. EFFECTIVE DIFFUSIVITY AND THERMOTRANSPORT

To begin with, we have to specify the theoretical frame relevant for the study of transport phenomena in the thermodiffusion configuration. It is quite difficult to derive a priori from thermodynamic considerations an expression relating the total mass flux  $J_M$  in purely diffusive conditions to the temperature and composition gradients. Various phenomenological expressions can be found in the literature, the most general being of the form

$$J_M = -\rho D \nabla C - \rho \mathcal{D}_T C (1 - C) \nabla T, \quad (2)$$

where  $\mathcal{D}_T$  is the thermodiffusion coefficient. When the induced concentration variations remain centered around a mean value  $C_0$ , Eq. (2) can be reduced to

$$J_M = -\rho D \nabla C - \rho D_T \nabla T, \quad (3)$$

with  $D_T = \mathcal{D}_T C_0 (1 - C_0)$ . In the case of dilute alloys the  $(1 - C)$  term in Eq. (2) can be dropped, yielding<sup>7</sup>

$$J_M = -\rho D \nabla C - \rho \mathcal{D}_T C \nabla T. \quad (4)$$

Finally, the thermodiffusion factor  $r = T^* (\mathcal{D}_T / D)$  can be introduced using statistical mechanics arguments. For isotopic solutions, this dimensionless factor would depend only on the atomic mass difference of the constituents and would thus be to the first order independent of the temperature.<sup>8,9</sup> In the presence of convection, an additional contribution,  $J = \rho C V$ , should be added in Eqs. (2)–(4).

We shall now proceed to estimate the error on the thermodiffusion coefficient induced by this contribution. Let us first consider, as done by Henry and Roux<sup>1,2</sup> that the mass flux is given by Eq. (3). For purely diffusive transport conditions, we see that at steady state,  $D_T$  is deduced from the product of the true diffusion coefficient  $D$  with the measured composition gradient  $G_D$  according to

$$D_T G_T + D G_D = 0, \quad (5)$$

$G_T$  being the applied axial thermal gradient. Let us now conjecture that, as in the isothermal case, the effect of convection can be accounted for via an effective coefficient  $D^*$ . The total mass flux for the thermotransport problem is given by

$$J_M^* = -\rho D^* \nabla C - \rho D_T \nabla T. \quad (6)$$

At steady-state, the relation between the thermal and solutal gradients is thus

$$D_T G_T + D^* G = 0. \quad (7)$$

In the above expression,  $G$  stands for the composition gradient in the presence of convection. Comparing Eqs. (5) and (7), we get

$$D G_D = D^* G. \quad (8)$$

It can be easily seen that Eq. (8) is consistent with the expected inequalities  $G_D \geq G$  and  $D^* \geq D$ . From Eq. (7), if one assumes wrongly purely diffusive conditions (i.e.,  $D^* = D$ ), an analysis of the raw composition data will lead to an effective value of  $D_T$ :

$$D_T^* = -D G / G_T. \quad (9)$$

From Eqs. (5) and (8), we get  $D^* G = D G_D = -D_T G_T$ , so that

$$D_T^* = (D / D^*) D_T. \quad (10)$$

Using Eq. (1), the above expression finally becomes

$$D_T^* = D_T / [1 + \alpha \bar{W}^2 H^2 / D^2]. \quad (11)$$

It should be noticed that we did not need to refer to the local form of the conservation equations to obtain Eq. (11); the key is to account for the convective contribution via an effective isothermal diffusion coefficient.

The predictions of Eq. (11) can now be compared to the Henry and Roux numerical results; it should be recalled that the computations related the composition gradient in the middle of the cavity normalized by its value for purely dif-

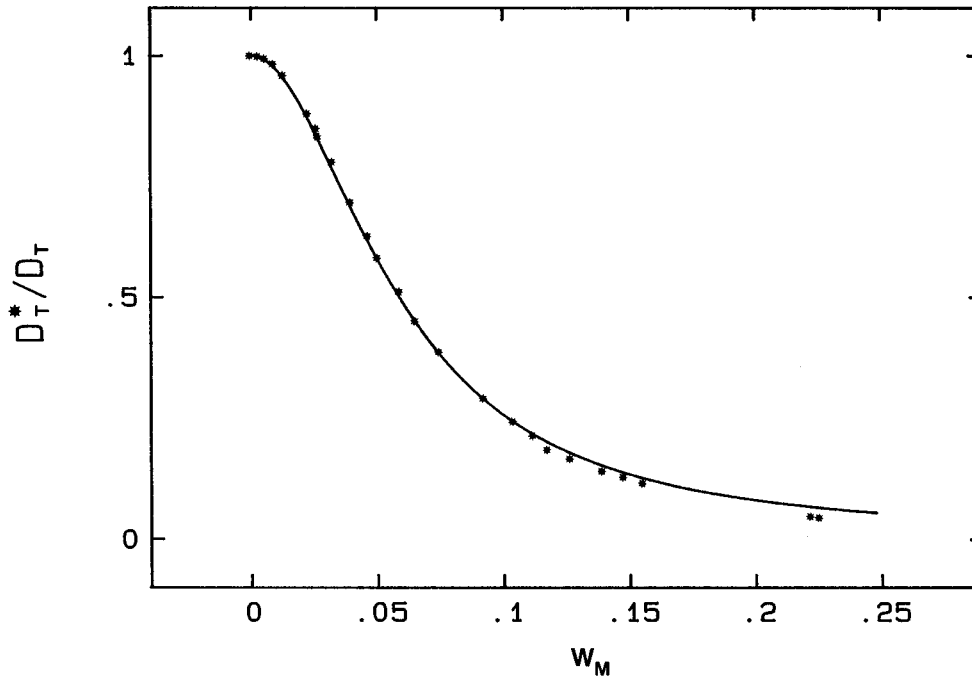


FIG. 1. Variation of the effective thermodiffusion coefficient with the convection velocity. Symbols: numerical data; full line: Eq. (15).

fusives conditions  $[(\partial X/\partial Z)_{\text{mid}}$  in their notations,  $G/G_D$  in ours] with the maximum convective velocity  $w_M$  in the fluid.

As the effective diffusivity approach features the average convective velocity, we have to find a relation between these two quantities. To do so, we can use the parallel flow solution proposed in Ref. 10 for cylindrical horizontal geometries (i.e. the configuration of Ref. 1) submitted to an axial temperature gradient. To the first order, the dimensionless axial velocity is given by

$$w = 0.125K_1(r^3 - r) \sin \vartheta. \quad (12)$$

The non-dimensional radial coordinate  $r$  being defined with respect to the radius of the capillary. The constant  $K_1$  stands for the temperature gradient and the position of a given point is given by its cylindrical coordinates  $r$  and  $\vartheta$ ,  $\vartheta$  being measured with respect to the horizontal.<sup>10</sup> Provided the body force remains constant along the cavity, which incidentally is a necessary condition for the existence of a parallel flow, the above solution can be generalized to the case where  $K_1$  accounts for both temperature and composition gradients. Simple algebra then leads to a relation between the average  $(\overline{|w|})$  and maximum ( $w_M$ ) convective velocities:

$$\overline{|w|}/w_M = 12\sqrt{3}/15\pi \approx 0.441. \quad (13)$$

From  $\overline{W} = (\nu/H)\overline{w}$ ,  $\overline{W}^2 H^2/D^2$  becomes  $\overline{w}^2 Sc^2$ ,  $Sc = \nu/D$  being the Schmidt number. Taking into account the fact that all the numerical simulations were carried out with  $Sc = 60$  and using Eqs. (8) and (10) to identify  $D_T^*/D_T$  with  $G/G_D$ , the prediction from Eq. (11) relating  $D_T^*/D_T$  and  $w_M$  can be written as

$$\frac{D_T^*}{D_T} = \frac{1}{1 + 700\alpha w_M^2}. \quad (14)$$

Shown in Fig. 1 is the variation of the normalized composition gradient with the maximum fluid velocity redrawn from Fig. 12 of Ref. 1, our notations  $D_T^*/D_T$  and  $w_M$  being used instead of  $(\partial X/\partial Z)_{\text{mid}}$  and  $\tilde{V}_{\text{max}}$ . The symbols are the numerical data points and the full line a curve of equation:

$$\frac{D_T^*}{D_T} = \frac{1}{1 + 290w_M^2}. \quad (15)$$

Equations (14) and (15) have similar forms and the agreement observed in Fig. 1 can be taken as a guarantee of the validity of our effective coefficient approach. To perfectly fit the Henry and Roux' data, we have set  $\alpha = 0.41$ . Such a value has the same order of magnitude as the  $\alpha = 1/11$  of the 2D numerical simulations of Ref. 4 or the  $\alpha = 0.25$  predicted by the scaling analysis. The discrepancy in terms of proportionality factors may seem quite large, but we think it can be ascribed to the nature of the modelling (2D versus 3D) and also to the physical problem (isothermal diffusion versus thermodiffusion).

At this point, one may question the interest of the effective diffusivity approach, since Jacqmin's solution<sup>3</sup> could account analytically for the Henry and Roux numerical results except at the extremities of the cavity. However, we think that our work brings some insight into the physics of the transport phenomena and we shall see in Secs. IV and V that the effective diffusivity formalism facilitates the discussion of the convective effects in experimental configurations.

Another advantage of this effective diffusivity formalism is that it allows us to generalize the above results to the other formulations of the thermodiffusion problem, namely Eqs. (2) and (4). In these cases, the analysis of the raw data will not feature directly the composition gradient. For instance,

with Eq. (4), the interested reader can check that the relevant variable is the quantity  $\log(C)$ .

However, whatever the formulation used, what is deduced from the temperature composition profile is always the ratio of the Soret and isothermal diffusion coefficients. The arguments developed in Eqs. (5) to (10) can be adapted at the expense of some algebra, and assuming that convective transport can be included in an effective diffusivity  $D^*$ , the analysis of the composition data assuming purely diffusive conditions will result in

$$\mathcal{S}_T^*/\mathcal{S}_T = D/D^*. \quad (16)$$

It should be noted that the result of Eq. (16) holds even though, as stated earlier, no parallel flow solution can be found in general since with formulations (2) and (4) the composition gradient in the cavity is not uniform. To sum things up, it appears that the sensitivity of a thermodiffusion coefficient measurement to convection does not depend on the formulation used, but only on the non-dimensional group  $\bar{W}^2 H^2 / D^2$ .

### III. EXPERIMENTAL RESULTS

The experiments carried out both on the ground and in microgravity were performed using the shear cell technique. We shall here only outline the basis of the method, the interested reader being referred to Ref. 5 for more details on the topic. The liquid samples are processed in thin capillaries of diameter 1–2 mm, which consist of a superposition of disks whose height ranges from 3 to 10 mm. The cell contains four capillaries and is itself installed in a closed cartridge filled with an inert gas; 100 mbar of He were used for the EURECA experiments. The disks are compressed by a spring in order to resist the vibrations and the accelerations of the spacecraft at launch.

An axial temperature gradient is established, and the thermotransport is allowed to proceed until a steady-state is reached. The liquid vein is then divided by differential rotation of its disks, and the material contained in each disk is left to solidify. The main advantage of the shear cell technique with respect to the standard procedure—where the sample is quenched at the end of the experiment—is that there is no solidification induced solutal segregation. Such a segregation can never be ruled out in practice and may lead to a significant bias in the analysis of the raw composition/temperature profile.

As can be expected, the time period necessary to reach a steady-state depends on the length of the liquid vein  $L$ . From the analytical solution obtained by de Groot<sup>7</sup> assuming purely diffusive transport conditions, it can be seen that the approach to equilibrium took place at a characteristic rate:

$$\tau = L^2 / \pi^2 D. \quad (17)$$

In practice, the separation can be considered quasi-complete at  $3\tau$ . In the Spacelab flights, the available microgravity time was limited to roughly six hours per experiment. This in turn limited the length of the samples to 18 mm, divided in six disks of 3 mm each. For the EURECA mission on the other hand, more than 250 hours of microgravity were available, which allowed us to increase the length of the capillary

TABLE I. Thermodiffusion factors  $r$  (see the text) in various tin based alloys for both microgravity and ground based experiments.

System	Composition (wt. %)	ground/ $\mu\text{g}$	$r (\times 10^{-3})$
Tin	isotopic		
	Sn <sup>112</sup>	ground	2 ± 12
	Sn <sup>112</sup>	$\mu\text{g}$ (EURECA)	77 ± 8
	Sn <sup>116</sup>	$\mu\text{g}$ (EURECA)	33 ± 12
Sn:Co	0.04	$\mu\text{g}$ (EURECA)	−55 ± 10
		ground	0 ± 20
Sn:Ag	0.04	$\mu\text{g}$ (FSLP)	1860 ± 40
		ground	47 ± 10
Sn:Bi	4	$\mu\text{g}$ (D1)	175 ± 40
		ground	−405 ± 10
Sn:Au	0.06	$\mu\text{g}$ (D1)	−758 ± 40
	0.07	ground	−182 ± 36
	6	$\mu\text{g}$ (EURECA)	−837 ± 12
		ground	−574 ± 50

vein to 110 mm, divided in 11 disks of 10 mm each. A better accuracy can thus be expected for the EURECA experiments.

After separation of the liquid vein and subsequent cooling, the material is removed from the disks and submitted to a neutronic flux in the SILOE reactor of the CEA-Grenoble. The composition of the samples can be deduced from a measurement of their  $\gamma$  activity. The sensitivity of such a method is of the order of ten parts per billion, and its accuracy in terms of relative concentration variations ranges from 0.1% to 0.5%, depending on autoabsorption and on cylindrical defects.

Various tin based alloys were examined with this technique. A necessary step in the analysis consists in identifying relevant absorption and disintegration reactions ( $\gamma$  energies, half lives) such as

$${}_{50}^{112}\text{Sn}(n, \gamma) {}_{49}^{113}\text{In}, \quad \gamma = 0.392 \text{ MeV}, \text{ 115 days,}$$

$${}_{50}^{116}\text{Sn}(n, \gamma) {}_{50}^{117}\text{Sn}, \quad \gamma = 0.159 \text{ MeV}, \text{ 14 days,}$$

$${}_{50}^{124}\text{Sn}(n, \gamma) {}_{51}^{125}\text{Sb}, \quad \gamma = 1.067 \text{ MeV}, \text{ 9.6 days,}$$

$${}_{27}^{59}\text{Co}(n, \gamma) {}_{27}^{60}\text{Co}, \quad \gamma = 1.173 \text{ MeV}, \text{ 5.3 years,}$$

$$\gamma = 1.332 \text{ MeV}, \text{ 5.3 years,}$$

$${}_{47}^{109}\text{Ag}(n, \gamma) {}_{47}^{110}\text{Ag}, \quad \gamma = 0.658 \text{ MeV}, \text{ 250 days,}$$

$${}_{79}^{197}\text{Au}(n, \gamma) {}_{79}^{198}\text{Au}, \quad \gamma = 0.41 \text{ MeV}, \text{ 2.7 days.}$$

It was unfortunately not possible to find an appropriate reaction for the bismuth doped tin alloy or for the other tin isotopes. As a consequence, a classical atomic adsorption technique had to be used to measure the Bi composition.

Our results are summarized in Table I in terms of the dimensionless thermodiffusion factor  $r$  defined as  $r = T^*(\mathcal{S}_T/D)$ . As can be seen from Eq. (4), at steady-state,  $r$  is given by the slope of the  $[\log(T), \log(C)]$  curve. The reported accuracy is simply the dispersion of the measurements. Even though the ground experiments were carried out

in a vertical set-up to *a priori* minimize the convection level, it appears that the separation observed in microgravity is always significantly higher.

The deduced thermodiffusion factor is in principle independent of the thermal field. In practice however, due to the relatively low values of  $r$ , the applied gradient should be high enough to yield observable composition variations. The difference between the end temperatures was 450 K for the EURECA flight, within an alumina cartridge. On the other hand, the previous microgravity experiments were run in a zirconia cartridge, with a 350 K temperature difference.

In all cases, the ground experiments shown in Table I were carried out in the same conditions as their flight counterparts, except that graphite was selected as cartridge material. We shall indeed see in Sec. V that the convective driving force in the Earth laboratory is associated with defects of the thermal field. In that respect, graphite appeared to be an interesting choice to smooth out all the unwanted temperature differences. Such a motivation did not exist for the microgravity experiments, as the details of the thermal field are not so important. Besides, as power is always severely limited aboard the spacecrafts, it would not have been possible to use a graphite cell.

#### IV. SORET COEFFICIENT MEASUREMENTS IN MICROGRAVITY

Using the formalism developed in Sec. II, we can proceed to a discussion of possible convective effects in microgravity conditions, our primary purpose being to assess whether thermodiffusion coefficient measurements can be safely carried out in space. There, the dominant convective driving force is given by the cross product interaction of the axial density gradient  $\nabla\rho$  with the transverse component of the residual gravity. We can thus again use the parallel flow solution proposed in Ref. 10, written here in dimensional form, to derive the average fluid velocity:

$$\bar{W} = (1/15\pi)(\nabla\rho/\rho_0)gH^3/\nu. \quad (18)$$

It should be once more noted that Eq. (18) is only valid when  $\nabla\rho$  is uniform in the cavity, which requires in our present problem that the formulation of Eq. (3) is used. However, we saw with Eq. (16) that the relative reduction of the value of the thermotransport coefficient induced by convection did not depend on the formulation. Our discussion can thus be safely based on Eq. (18).

The equation of state of the fluid being  $\rho = \rho_0[1 - \beta_T(T - T_0) + \beta_S(C - C_0)]$  we get from Eq. (9),

$$\nabla\rho/\rho_0 = -\beta_T G_T + \beta_S G = -[\beta_T + (D_T^*/D)\beta_S]G_T. \quad (19)$$

As noted in Ref. 1, depending on the signs of  $\beta_S$  and  $D_T^*$ , thermotransport will lead to an acceleration or a damping of the flow. The effective coefficient  $D_T^*$  should *a priori* be used in Eq. (19) to account for the actual solutal effect. Under the assumption of volume additivity, reasonable for liquid systems, the solutal expansion coefficient can be estimated from the formula giving the mass density of an A-B alloy:

$$\rho = \rho_A \rho_B / (x_B \rho_A + x_A \rho_B), \quad (20)$$

where  $x_A, \rho_A, x_B, \rho_B$  are the mass fractions and mass densities of the elements A and B. Simple algebra indicates that  $\beta_S$  will vary between  $\rho_A/\rho_B - 1$  and  $\rho_B/\rho_A - 1$ .

The difference between the mass densities of the constituents A and B may be quite high in liquid metals, and  $\beta_S$  can take values, expressed in inverse weight fraction, ranging from 0.1 to 2. On the other hand,  $\beta_S$  is much smaller in semiconductor alloys of the same class (III-V, II-VI), typically of the order of 0.05, with the exception of germanium in silicon ( $\beta_S = 1.2$ ).

In dilute tin based alloys, the solutal contribution in Eq. (19) can be safely omitted; indeed, the ratio  $D_T/D$  is proportional to the average solute concentration  $C_0$  and does not exceed  $10^{-5}$  (wt. fr)  $\text{K}^{-1}$  for  $C_0$  smaller than 0.01 wt. fr.<sup>5</sup> Using typical values for the thermal expansion coefficient  $\beta_T = 10^{-4} \text{K}^{-1}$ , the applied temperature gradient  $G_T = 10^4 \text{Km}^{-1}$ , the fluid viscosity  $\nu = 2 \times 10^{-7} \text{m}^2 \text{s}^{-1}$ , the isothermal diffusion coefficient  $D = 5 \times 10^{-9} \text{m}^2 \text{s}^{-1}$  and the capillary diameter  $H = 1.5 \times 10^{-3} \text{m}$ , Eq. (18) leads to

$$\bar{W}H/D = 1050(g/g_0), \quad (21)$$

where the ratio  $g/g_0$  measures the reduction of the gravity level aboard the spacecraft with respect to Earth based conditions. Even in a manned mission, this ratio very rarely exceeds  $10^{-4}$ , its typical value being in the  $[10^{-5}, 10^{-6}]$  range, so that in any case  $\bar{W}H/D \leq 0.1$ . From Eq. (11), it appears clearly that the convection induced error on the Soret coefficient will be very small, since the proportionality factor  $\alpha$  was seen to be always smaller than unity.

The discussion up to this point has been based on Eq. (18), which comes from a parallel flow solution obtained in a constant gravity vector configuration. In space, gravity fluctuates both in direction and magnitude and the developments of this section are only valid *stricto sensu* for dc  $g$ -levels. However, these dc  $g$ -levels are the ones that impact most on solute transport, since it can be shown that high frequency gravity variations are damped by viscosity.<sup>11</sup>

In concentrated alloys, the solutal and thermal contributions in Eq. (19) can be of the same order of magnitude, but it can again be stated that the space experiments take place under purely diffusive transport conditions. However, even in dilute metallic or semiconducting systems, the capillary diameter should be limited to roughly 2 mm, due to the  $H^4$  dependence of  $\bar{W}H/D$ .

#### V. SORET COEFFICIENT MEASUREMENTS ON EARTH

Our purpose in this section is to discuss the possibility of performing relevant Soret coefficient measurements on Earth, relying again on the formalism developed in Sec. II. We shall also see that our experimental results in tin based alloys and the numerical data of the Henry and Roux support the validity of our effective diffusivity approach.

In order to minimize convective effects, it appears natural to maintain the set-up in a vertical position, with the higher temperature at the top of the sample, but these precautions may not be sufficient to guarantee purely diffusive solute transport. Indeed, a slight misalignment of the capil-

lary axis with the local vertical gives birth to fluid motion, due to the non-zero value of the cross product of the imposed axial temperature gradient with gravity.

Another possible cause for convection is related to the overall heat transfer in the experimental set-up. Indeed, when the thermal conductivities of the sample and the surrounding medium are different, the heat flow from the hot end to the cold end can not be purely directional, resulting in temperature gradients inside the capillary. In practice, these gradients will always contribute to the convective flow.

The identification of the dominant mechanism is far from obvious as both causes are very difficult to appreciate. Indeed, typical misalignments are probably smaller than  $1^\circ$ , but a precise measurement of the angle is hardly possible. Similarly, in an optimized set-up, the radial temperature differences are very low, of the order of 0.1 K; an accurate estimation, for instance with the help of numerical simulations, would be very difficult.

Another phenomenon to take into account is the solutal stabilization of the flow, as discussed by Hart.<sup>6</sup> Briefly stated, in a vertical set-up, when the heavier component diffuses downwards, the convection induced radial segregation tends to decrease the radial density gradient and thus the fluid velocity. A discussion of this effect had been proposed in a former paper by one of us,<sup>5</sup> but we shall have to come back on this point.

To start with, let us check the potential effect of a misalignment of the capillary in a dilute system. The discussion can again be based on Eq. (18), provided that  $g$  is changed to  $g \sin \alpha$ ,  $\alpha$  being the deflection angle with the vertical. Using the same values as before,  $\beta_T = 10^{-4} \text{ K}^{-1}$ ,  $G_T = 10^4 \text{ Km}^{-1}$ ,  $\nu = 2 \times 10^{-7} \text{ m}^2 \text{ s}^{-1}$ ,  $D = 5 \times 10^{-9} \text{ m}^2 \text{ s}^{-1}$  and  $H = 1.5 \times 10^{-3} \text{ m}$ , Eq. (18) leads to

$$\bar{W}H/D = 1050 \sin \alpha. \quad (22)$$

To keep  $\bar{W}H/D$  below 0.5,  $\alpha$  has to remain smaller than  $0.03^\circ$ , which is hardly possible in practice. A reduction of the

capillary diameter to 1 mm would increase the allowed misalignment to  $0.14^\circ$ , which is still a very stiff requirement.

The estimation of the error related to radial temperature gradients is more complex, since the driving force can not be considered uniform in general. However, let us assume for the present discussion that Eq. (18) can again be used. The typical dimension of the cavity  $H$  should now be taken as the capillary radius, due to the symmetry of the heat flux along the sample. Setting  $H = 7.5 \times 10^{-4} \text{ m}$  and keeping the other values as before, we get

$$\bar{W}H/D = 6.6 \times 10^{-3} G_{T,r}. \quad (23)$$

The radial thermal gradient  $G_{T,r}$  is given as  $G_{T,r} = \Delta T_r / H$ ,  $\Delta T_r$  being a relevant temperature difference. To keep  $\bar{W}H/D$  below 0.5 requires  $G_{T,r}$  smaller than 75 K/m, which translates into  $\Delta T_r \leq 5.7 \times 10^{-2} \text{ K}$  over a 0.75 mm capillary. Such low values are very difficult to obtain in practice considering the large axial gradients necessary to get an observable thermotransport separation.

In concentrated alloys, we found that a stabilizing solute gradient could reduce significantly the convection related transport. To do so, we estimated the velocity reduction due to the stabilization effect. This was done in Ref. 12, where we derived a damping factor  $\zeta$  as

$$\zeta = \bar{W} / \bar{W}(\text{Ra}_S = 0), \quad (24)$$

using Hart's analytical solution<sup>6</sup> for the flow in a long cavity submitted to both temperature and composition gradients. In the above expression,  $\text{Ra}_S$  is the solutal Rayleigh number,  $\text{Ra}_S = \beta_S g G H^4 / \nu D$ , that measures the amount of solutal stabilization and  $\bar{W}(\text{Ra}_S = 0)$  is the average velocity of the thermally driven flow. More precisely, setting  $M = (-\text{Ra}_S/4)^{-1/4}$ , we found<sup>12</sup>

$$\zeta = \frac{96}{M^4} f(M), \quad (25)$$

with  $f(M)$  equal to

$$\frac{|\sinh(M/2)\cosh(M/2) + \sin(M/2)\cos(M/2) - \sinh(M/2)\cos(M/2) - \sin(M/2)\cosh(M/2)|}{|\sinh(M/2)\cosh(M/2) + \sin(M/2)\cos(M/2)|}.$$

However, our numerical simulations<sup>12</sup> showed that the damping effect deduced using the effective diffusion approach in connection with Hart's model was overestimated when the stabilizing gradient was high, and that the attainment of diffusion controlled conditions on the ground was not possible in practice.

This came as a contradiction to the conjecture made a few years ago<sup>5</sup> that for the Sn: 6 wt. % Au alloy, solutal stabilization could be strong enough to guarantee purely diffusive transport conditions even in the Earth's gravity. However, the discussion of Ref. 5 relied on a derivation of the damping effect that our more recent results<sup>12</sup> proved to be overestimated. Besides, the results of the EURECA experiment showed that the separation was higher in space, indi-

cating that natural convection was indeed a factor on the ground.

To finish with, it is interesting to see whether the Henry and Roux numerical results, coming from a modelling of a microgravity configuration,<sup>1</sup> could account, at least qualitatively, for the reduced separation observed on Earth for various solutes in tin. In that case, the missing link will of course be provided by our effective diffusivity approach. First, let us notice that from the discussion in Sec. II, the ratio  $r(1g)/r(\mu g)$  can be identified with  $D_T^*/D_T$ .

Unfortunately, we do not have accurate measurements for neither the set-up misalignment with the vertical, nor for the lateral temperature differences in the capillary (rough estimates indicate that the value of these defaults could be of

TABLE II. Variation of the thermodiffusion factor ratio  $r(1g)/r(\mu g) = D_T^*/D_T$  with sample diameter and stabilizing effect.

Experiment	Sample diameter (mm)	$r_{1g}/r_{\mu g}$	Stabilizing effect
0.04 wt. % Co	2	0	No
0.04 wt. % Ag	1.5	0.27	No
0.06 wt. % Au	1.5	0.22	No
4 wt. % Bi	1.5	0.53	Yes
6 wt. % Au	1.5	0.69	Yes

the order of  $0.5^\circ$  and  $0.2$  K, respectively). It is thus not possible to derive the absolute value of  $w_M$  in the experiments. Only the relative magnitudes of the convection velocity from one experiment to another can be estimated with the help of Hart's model.

We thus have to select a reference experiment before deriving a damping or acceleration factor for the others. To do so, the best choice is to use the dilute system Sn: 0.04 wt. % Ag and Sn: 0.06 wt. % Au where the effect of solutal stabilization can safely be neglected. As can be seen in Table II, the ratio of the thermodiffusion factors is close to 0.25 in both cases. For tin isotopes,  $r(1g)/r(\mu g)$  should also be around 0.25, but we think that the absence of separation observed on the ground is mainly due to the difficulty of measuring very limited composition variations.

Reporting the reference Sn: 0.04 wt. % Ag and Sn: 0.06 wt. % Au experiments on the curve represented in Fig. 1, we see that the dimensionless fluid velocity  $w_M$  corresponding to the observed separation [ $r(1g)/r(\mu g) \approx 0.25$ ] is of the order of 0.1. We cannot tell whether the dominant driving force is related to a misalignment of the set-up or to existing tem-

perature gradients in the capillary, but the important point for our present purposes is that we can use  $w_M = 0.1$  as a reference velocity.

Figure 2 represents the variation of the effective thermodiffusion coefficient with fluid velocity as obtained from Eq. (15) for a larger  $w_M$  range than in Fig. 1. It appears that for the Sn:Co experiment  $w_M$  is of the order of 0.32, due to the  $H^4$  dependence of the convective level on the diameter. As seen in Fig. 2, this means that the predicted thermodiffusion factor ratio  $r(1g)/r(\mu g)$  will be very close to zero, in agreement with the experiments, where no separation could be observed on the ground.

The comparison between numerical modelling and experiment for the Sn: 4 wt. % Bi and the Sn: 6 wt. % Au systems can be done via a derivation of the damping factor derived in Eq. (25). From Eq. (4), the relevant solutal gradient to be used in  $Ra_S$  is given by  $G = (r/\bar{T})\bar{C}G_T$ . In our experiments,  $\bar{T}$ , the mean temperature in the capillary, is roughly 800 K.

For the Sn:Au system, using  $\beta_S = 6.1 \times 10^{-3} (\text{wt. \%})^{-1}$ ,  $\nu = 1.8 \times 10^{-7} \text{ m}^2 \text{ s}^{-1}$ ,  $D = 5 \times 10^{-9} \text{ m}^2 \text{ s}^{-1}$ ,  $r = -0.837$  and experimental conditions  $G_T = 10^4 \text{ Km}^{-1}$ ,  $H = 7.5 \times 10^{-4} \text{ m}$ ,  $C = 6 \text{ wt. \%}$ , we get  $G = -68 \text{ wt. \% m}^{-1}$ ,  $Ra_S = -1460$  and from Eq. (25),  $\zeta = 0.25$ . For the Sn:Bi alloy, keeping the same values for  $\nu$ ,  $D$ ,  $G_T$  and  $H$ , but with  $r = -0.758$  and  $C = 4 \text{ wt. \%}$ , we find  $G = -32 \text{ wt. \% m}^{-1}$ ,  $Ra_S = -337$  and  $\zeta = 0.59$ .

As stated earlier, the damping effect estimated from Eq. (25) was found to be overestimated at high values of  $Ra_S$ .<sup>12</sup> However, at moderate  $Ra_S$  numbers ( $Ra_S = -1460$  and  $Ra_S = -337$ ), we could expect  $\zeta$  to be accurately predicted from Eq. (25). Indeed, reporting the points corresponding to the Sn: 4 wt. % Bi and the Sn: 6 wt. % Au experiments on

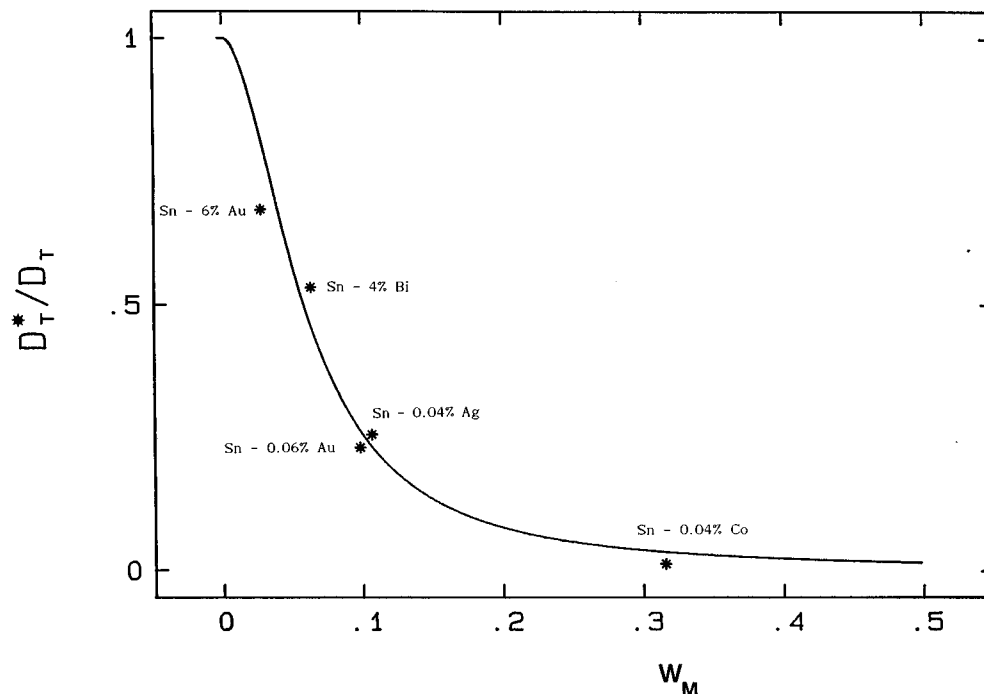


FIG. 2. Effect of convection in ground based Soret coefficient measurements of various tin based alloys [full line: Eq. (15)]. Dilute systems Sn: 0.04 wt. % Ag and Sn: 0.06 wt. % Au were taken as a reference to estimate the relevant  $w_M$ .



the curve of Fig. 2, we find that they compare fairly well with the predictions of Henry and Roux. Considering the large number of simplifying assumptions, it is gratifying to see that the numerical simulations can account for the observed separations.

The present result clearly demonstrates that the attainment of diffusion controlled conditions is virtually impossible on Earth in our experimental configuration. It also supports the validity of the effective diffusivity approach as a tool for a physical understanding of the transport phenomena in the fluid.

#### IV. CONCLUDING REMARKS

Our purpose in this work was to gain some insight into the problem of natural convection perturbations in Soret coefficients measurements. We first saw that an effective diffusivity concept, similar to the one introduced in an earlier paper for isothermal configurations<sup>4</sup> was applicable to thermodiffusion. The scaling analysis carried out indicates that the measurement error induced by convection is proportional to the square of the fluid velocity. We found that this effective diffusivity concept compared well with the 3D numerical simulations of Henry and Roux.<sup>1</sup>

We then proceeded to a presentation of our experimental results from both past microgravity missions<sup>5</sup> and the recent EURECA flight on tin based alloys. We found that the solutal separation, and thus the deduced Soret coefficient, was always significantly higher in space, even in systems where solutal stabilization of the flow was certainly a factor.

To account for such a result, we analyzed the possibility of realizing clean, error free measurements both on the ground and in microgravity in liquid metals or semiconductors. Taking the worst case of manned space flights where the gravity level can reach  $10^{-4} g_0$ , it appeared that convective interference could be safely ruled out in all space experiments, provided that the capillary diameter did not exceed 2 mm. The potential of microgravity is also clear for the case of organic mixtures and aqueous solutions.<sup>13</sup>

On the other hand, convective transport was found to be hardly avoidable on Earth, even in an optimized configuration. The requirements in terms of both misalignment of the set-up with the vertical and lateral temperature gradients were seen to be much too stiff in practice. The application of a magnetic field could be an interesting possibility to reduce the fluid velocity in liquid metals or semiconductors, but whether purely diffusive transport conditions could be attained remains questionable.

Finally, we discussed the difference between our ground and microgravity results in tin based alloys using Hart's model for solutal stabilization of the flow. It appeared that convective transport could never be totally eliminated, even in systems where damping was efficient. We also showed that the Henry and Roux numerical simulations could qualitatively account for the reduced separation observed experimentally on Earth.

#### ACKNOWLEDGMENTS

The present work was carried out in the frame of the GRAMME agreement between the Centre National d'Etudes Spatiales and the Commissariat à l'Énergie Atomique. It is a pleasure to thank D. Henry for numerous fruitful discussions on the topic. The help of D. Beretz, J. C. Royer and their team with the measurements of neutronic activities in the SILOE facility of the CEA-Grenoble is also gratefully acknowledged.

#### APPENDIX: THE DERIVATION OF THE EFFECTIVE DIFFUSION COEFFICIENT

The expression relating the effective and true isothermal diffusion coefficients [Eq. (1) in the text] was first published in Ref. 4, but our purpose here is to propose a more elegant derivation, that allows a better identification of the relevant physical mechanisms and of the assumptions required. To start with, let us consider the classical convecto-diffusive solute conservation equation:

$$\frac{\partial C}{\partial t} + (V \cdot \nabla)C = D\nabla^2 C, \quad (\text{A1})$$

where  $V$  stands for the fluid velocity and  $D$  for the isothermal diffusion coefficient. A key step in the derivation consists in focusing only on the laterally averaged concentration field, since in most experimental configurations, e.g. for the shear cell or long capillary techniques, it is the variable used in the analysis procedure. Let us thus distinguish the axial and radial variations in the overall composition field:

$$C(x, y, z, t) = C_0(z, t) + C_1(x, y, z, t),$$

$$C_0(z, t) = \langle C \rangle_S,$$

$\langle \rangle_S$  representing the lateral average over the capillary cross section. The capillary is oriented along the  $z$ -axis in our choice of notations. With these definitions,  $C_1$  can be considered as a fluctuation superimposed to the mean composition  $C_0$ . Let us now proceed to take the average of the three terms in Eq. (A1):

$$\left\langle \frac{\partial C}{\partial t} \right\rangle_S = \frac{\partial C_0}{\partial t}, \quad (\text{A2a})$$

$$\langle (V \cdot \nabla)C \rangle_S = \frac{\partial \langle WC \rangle_S}{\partial z}, \quad (\text{A2b})$$

$$\langle D\nabla^2 C \rangle_S = D \frac{\partial^2 C_0}{\partial z^2}, \quad (\text{A2c})$$

$W$  standing for the  $z$ -component of the fluid velocity. The no-slip condition at the boundaries and the continuity equation for an incompressible fluid were invoked to derive Eq. (A2b). As for Eq. (A2c), the only assumption required is that of no solutal flux on the lateral edges,  $\partial C / \partial n = 0$ , with  $n$  standing for the normal to the capillary in the  $(x, y)$  plane. Taking advantage of the zero net mass flux in the  $z$ -direction, Eq. (A2b) can be transformed to yield  $\langle WC \rangle_S = \langle WC_1 \rangle_S$ . Equation (A1) then becomes

$$\frac{\partial C_0}{\partial t} + \frac{\partial(\langle WC_1 \rangle_S)}{\partial z} = D \frac{\partial^2 C_0}{\partial z^2}. \quad (\text{A3})$$

The reader should be convinced that no approximations are involved in the derivation of Eq. (A3). The problem is that we need to get some informations on  $C_1$  to find a solution in terms of  $C_0$ . To do so, let us subtract Eq. (A3) from Eq. (A1). The result reads as

$$\frac{\partial C_1}{\partial t} + (V \cdot \nabla)C_0 + (V \cdot \nabla)C_1 - \frac{\partial(\langle WC_1 \rangle_S)}{\partial z} - D\nabla^2 C_1 = 0. \quad (\text{A4})$$

From now on, a few hypotheses are required; first, we shall assume the convection induced perturbation of the solute field  $C_1$  to be small, such that the terms  $(V \cdot \nabla)C_1$  and  $\partial(\langle WC_1 \rangle_S)/\partial z$  can be considered second order compared to  $(V \cdot \nabla)C_0 = W\partial C_0/\partial z$ . Equation (A4) then becomes

$$\frac{\partial C_1}{\partial t} + W \frac{\partial C_0}{\partial z} - D\nabla^2 C_1 = 0. \quad (\text{A5})$$

Due to the long duration and the large extent in the  $z$ -direction of the capillary in typical experimental configurations, one can also suppose the time and  $z$ -variations of  $C_1$  to be negligible with respect to the lateral derivation terms, yielding

$$D\nabla_S^2 C_1 = W \frac{\partial C_0}{\partial z}, \quad (\text{A6})$$

$\nabla_S^2$  representing the Laplacian operator in the capillary cross section. In principle,  $C_1$  can be exactly deduced from Eq. (A6) and adequate boundary conditions. However, the derivation of an approximate solution will facilitate the identification of the relevant physical parameters of the problem. Indeed, after multiplication by  $C_1$  of both sides of Eq. (A6) and lateral averaging of the obtained expression, we find

$$\langle WC_1 \rangle_S \frac{\partial C_0}{\partial z} = -D \langle \nabla_S C_1 \cdot \nabla_S C_1 \rangle_S. \quad (\text{A7})$$

All we now have to do is to find an ‘‘order of magnitude’’ solution for  $\nabla_S C_1$  to get an estimate of the expression in the left hand side of Eq. (A7). To do so, let us assume that there exists a direction in the cross section, denoted  $\xi$  in the following, where the composition variations are the strongest. Equation (A6) can then be written as

$$D \frac{\partial^2 C_1}{\partial \xi^2} = W \frac{\partial C_0}{\partial z}. \quad (\text{A8})$$

The variable  $\xi$  is supposed to range from  $-H/2$  to  $+H/2$ ,  $H$  being a typical dimension of the capillary cross section. Integration of Eq. (A8) over the half cavity where  $W$  is positive, taken here as  $[-H/2, 0]$ , we find

$$D \left. \frac{\partial C_1}{\partial \xi} \right|_0 = (H/2) \bar{W} \frac{\partial C_0}{\partial z}, \quad (\text{A9})$$

$\bar{W}$  standing for the lateral average of  $W$ . For order of magnitude purposes, it is certainly licit to assume that the  $C_1$  gradient remains uniform in the cross section and close to  $\partial C_1/\partial \xi|_0$ . Equation (A7) then yields

$$D \langle WC_1 \rangle_S = \left( \frac{H^2}{4} \right) \bar{W}^2 \frac{\partial C_0}{\partial z}. \quad (\text{A10})$$

Reporting Eq. (A10) in Eq. (A3), we see that our initial solute conservation equation becomes

$$\frac{\partial C_0}{\partial t} = D^* \frac{\partial^2 C_0}{\partial z^2}, \quad (\text{A11})$$

where the effective diffusion coefficient  $D^*$  is given as

$$D^* = D [1 + (1/4)(\bar{W}^2 H^2 / D^2)]. \quad (\text{A12})$$

Equation (A11) states that it is impossible to differentiate between a convecto-diffusive and a purely diffusive transport process, provided that  $D$  is changed to  $D^*$ . Of course, the various assumptions made in the course of the derivation limit the range of applicability of such a result to the present problem. More specifically, the key step in the procedure appears to be the averaging of the composition field over the capillary cross section, which allows convection to hide in the pretense of accelerated diffusion.

<sup>1</sup>D. Henry and B. Roux, ‘‘Three dimensional numerical study of convection in a cylindrical thermal diffusion cell: Its influence on the separation of constituents,’’ *Phys. Fluids* **29**, 3562 (1986).

<sup>2</sup>D. Henry and B. Roux, ‘‘Three dimensional numerical study of convection in a cylindrical thermal diffusion cell: Inclination effect,’’ *Phys. Fluids* **30**, 1656 (1987).

<sup>3</sup>D. Jacqumin, ‘‘Parallel flows with Soret effect in tilted cylinders,’’ *J. Fluid Mech.* **211**, 355 (1990).

<sup>4</sup>J. P. Garandet, C. Barat, and T. Duffar, ‘‘On the effect of natural convection in mass transport measurements in dilute liquid alloys,’’ *Int. J. Heat Mass Transfer* **38**, 2169 (1995).

<sup>5</sup>J. P. Praizey, ‘‘Benefits of microgravity for measuring thermotransport in liquid metallic alloys,’’ *Int. J. Heat Mass Transfer* **32**, 2385 (1989).

<sup>6</sup>J. E. Hart, ‘‘On sideways diffusive instability,’’ *J. Fluid Mech.* **49**, 279 (1971).

<sup>7</sup>S. R. de Groot, ‘‘Théorie phénoménologique de l’effet Soret,’’ *Physica* **9**, 699 (1942).

<sup>8</sup>R. Clark Jones, ‘‘On the theory of the thermal diffusion coefficient for isotopes,’’ *Phys. Rev.* **58**, 111 (1940).

<sup>9</sup>S. Chapman and T. G. Cowling, *The Mathematical Theory of Non-Uniform Gases* (Cambridge University Press, Cambridge, 1952).

<sup>10</sup>A. Bejean and C. L. Tien, ‘‘Fully developed natural counterflow in a long horizontal pipe with different end temperatures,’’ *Int. J. Heat Mass Transfer* **21**, 701 (1978).

<sup>11</sup>D. Thevenard and H. Ben Hadid, ‘‘Low Prandtl number convection in a rectangular cavity with longitudinal thermal gradient and transverse  $g$ -jitters,’’ *Int. J. Heat Mass Transfer* **34**, 2167 (1991).

<sup>12</sup>C. Barat and J. P. Garandet, ‘‘The effect of natural convection in liquid phase mass transport coefficient measurements: The case of thermosolutal convection,’’ *Int. J. Heat Mass Transfer* **39**, 2177 (1996).

<sup>13</sup>S. Van Vaerenbergh, J. C. Legros, and J. C. Dupin, ‘‘First results of Soret coefficient measurement experiment,’’ *Adv. Space Res.* **16**, 69 (1995).